Full Paper

Propellants, Explosives, Pyrotechnics

DOI: 10.1002/prep.201300018

Preparation and Properties Study of Core-Shell CL-20/TATB Composites

Zhijian Yang,*[a] Jinshan Li,[a] Bing Huang,[a] Shijun Liu,[a] Zhong Huang,[a] and Fude Nie[a]

Abstract: The insensitive high explosive 1,3,5-triamino-2,4,6-trinitrobenzene (TATB) was selected for coating and desensitization of hexanitrohexaazaisowurtzitane (CL-20), another high explosive, after surface modification. About 2 wt-% polymer binder was adopted in the preparation process to further maintain the coating strength and fill the voids among energetic particles. The structure, sensitivity, polymorph properties, and thermal behavior of CL-20/TATB by coating and physical mixing were studied. Scanning electron microscopy (SEM) and X-ray photoelectron spectroscopy (XPS) results indicate that submicrometer-sized TATB was compactly coated onto the CL-20 surface with coverage close to 100%. The core-shell structure of CL-20/TATB was confirmed by observation of hollow TATB shell from the CL-20 core dissolved sample. X-ray diffraction (XRD) analysis revealed that the polymorph of CL-20 maintained ε form during the whole preparing process. Thermal properties were studied by thermogravimetry (TG) and differential scanning calorimeter (DSC), showing effects of TATB coating on the polymorph thermal stability and exothermic decomposition of CL-20. Both the impact and friction sensitivities were markedly reduced due to the cushioning and lubricating effects of TATB shell. The preparation of explosive composites with core-shell structure provides an efficient route for the desensitization of high explosives, such as CL-20 in this study.

Keywords: Core-shell structure · CL-20 · TATB · Coating · Desensitization

1 Introduction

Improving the safety and effective destructibility of munitions is a long-term target for the development of modern weapons. Unfortunately, existing explosives with good performance usually have poor thermal and mechanical stability, and vice versa. Hexanitrohexaazaisowurtzitane (CL-20, HNIW), firstly synthesized by Nielsen [1], is a high energy density material (HEDM) of considerable interests for a variety of applications [2–5], especially for military purpose [6]. The energy output of CL-20 is proved to be 10–15% higher than cyclotetramethylenetetranitramine (HMX). The propellants or explosive composites containing CL-20 are expected to improve the performance in specific impulse, burn rate, detonation pressure, and detonation velocity [7–9]. However, there are strong limitations for the application of CL-20 in weapon systems. These limitations are caused by its high sensitivity towards impact, friction, and electric spark. Typical approaches to reduce the sensitivity of CL-20 include decreasing the particle size [10–12], removing the impurities/defects by recrystallization [13–15], preparing energetic cocrystals [16–18] and exploring the polymer bonded explosives (PBXs) [19,20]. Among them, the techniques based on solution crystallization are largely restricted in reducing the sensitivity of such high explosives, due to non-changing of the inherent molecules or components. Also, the production scale of energetic cocrystals is difficult to amplify for engineering applications. Up to now, most efforts have been devoted to study the CL-20 based PBXs, such as LX-19, PAX-12, PAX-11, PAX-29, DLE-CO38 and PBXW-16 as reported previously [20–22]. It was found that the uniform coating of some insensitive agents on the surface provides an effective route to the desensitization of CL-20 based composites. Nevertheless, large-scale use of inert additives was essential to meet the safety requirements in PBXs, which will lead to the apparent energy loss.

To reduce the sensitivity but retain high energy density, an exploration of core-shell structure by coating the insensitive explosives onto the surface of sensitive explosives seems rather attractive. Systems such as HMX/NTO [23–26], HMX/TATB [27,28], RDX/TNT [29], HMX/TNT [30] etc. have shown a significant decrease in sensitivity. It is hoped that an integral core-shell structure will have the energy density of the core and the sensitivity of the shell. However, the most serious problem is the self-nucleation of the shell materials during the crystallization coating process. In that situation, coated HMX crystals should be filtered using a sieve to remove the self-nucleated NTO particles [25], leading to the low utilization of shell material. Besides low coverage and weak coating strength, the thickness of the shell layer

[a] *Z. Yang, J. Li, B. Huang, S. Liu, Z. Huang, F. Nie*
Institute of Chemical Materials
China Academy of Engineering Physics
Mianyang 621900, Sichuan, P. R. China
**e-mail: zhijianyang@yahoo.com.cn*

is difficult to control. In view of the above, an intensive study of energetic-energetic core-shell structures is warranted.

It is well known that 1,3,5-triamino-2,4,6-trinitrobenzene (TATB) is a moderately powerful, thermally stable, insensitive high explosive (IHE), which is favorable to prepare insensitive munitions. In this work, we report the first example of uniform coating of TATB on the surface of CL-20 crystals to form a compact core-shell structure. Both the SEM and XPS results indicated that submicrometer-sized TATB particles were compactly coated onto the CL-20 surface with coverage close to 100%. The mechanical sensitivity of such composites was markedly reduced. The phase transition and thermal properties were investigated by XRD and TG/DSC. And the facile preparation method for core-shell CL-20/TATB also endows their potential engineering amplification.

2 Experimental

2.1 Materials

CL-20 was provided by Liaoning Qingyang Chemical Industry Co., Ltd. TATB (purity 99%, particle size about 800 nm) was provided by Institute of Chemical Materials, CAEP, China, it was obtained through a jet milling method. The other chemicals and reagents used in the presented study were commercially purchased and used without further purification.

2.2 Purification of CL-20

The purification process was carried out by a solvent/non-solvent recrystallization method. CL-20 (45 g) was added into ethyl acetate (120 mL) typically, the solution was collected by filtration after complete dissolution to remove the insoluble impurities, including some organic precursors for the synthesis of CL-20 and inorganic compounds. Afterwards, toluene (400 mL) was added in drops to the solution under continuous stirring. Pure ε-CL-20 products were obtained after filtration and drying.

2.3 Preparation of Core-Shell CL-20/TATB

CL-20 (30 g) was added to H_2O (50 mL) and dispersed whilst stirring. About 0.01 mg of surfactant such as polyvinyl alcohol (PVA) or polyoxyethylenesorbitan monolaurate (Tween-20) was used as the surface modification agent, followed by the addition of a certain amount (5 to 55 wt-% of the total weight of products) of TATB treated with ultrasonic dispersion in water beforehand. Afterwards, 0.5 to 5 wt-% polymer binder solution such as Estane 5703 (poly [ester urethane] block copolymer) or EVA (ethylene-vinyl acetate copolymer) was added dropwise, the system was heated to 60 °C in a vacuum. After removing the organic solvent, the precipitate was filtered, washed, and dried in air to give core-shell CL-20/TATB composites. In addition, the physical mixtures of CL-20 and TATB with the same molar ratio were prepared and used as a reference.

2.4 Characterization

Scanning electron microscopy (SEM) measurements were performed with a LE0438 VP instrument at an operating voltage of 25 kV. X-ray diffraction (XRD) patterns were recorded with a Rigaku D/Max-rB 12 kW diffractometer (Cu-K_α). Fourier-transform infrared (FT-IR) spectra were collected with a Nicolet Fourier Spectrophotometer-360 using KBr pellets. Thermogravimetry (TG) test was recorded with a TA Q600 instrument and the differential scanning calorimeter (DSC) test was recorded with a TA Q100 instrument from 25 to 500 °C in a nitrogen (50 mL min^{-1}) atmosphere with ramp of 10 °C min^{-1}. X-ray photoelectron spectroscopy (XPS) was conducted on a VG ESCALAB 250 instrument, with Mg-K_α radiation at 200 W.

2.5 Sensitivity Test

The impact sensitivity test was conducted with a WL-1 type impact sensitivity instrument according to GJB-772A-97 standard method 601.2 [31]. The test conditions are: drop weight, 2 kg; sample mass, 30 mg. The impact sensitivity of each test sample was expressed by the drop height of 50% explosion probability (H_{50}).

The friction sensitivity test was determined on a WM-1 type friction sensitivity instrument according to GJB-772A-97 standard method 602.1 [31]. The test conditions are: relative pressure, 3.92 MPa; sample mass: 30 mg, pendulum weight: 1.5 kg; pendulum angle: 90 °. The fraction sensitivity of each test sample was expressed by explosion probability (P).

3 Results and Discussion

3.1 Morphological and Structural Features of Core-Shell CL-20/TATB

Figure 1 shows the SEM images of CL-20 and core-shell CL-20/TATB samples. The size distribution of CL-20 after purification is uniform, with the average particle size of about 80 μm and smooth surface (Figure 1a). The CL-20 crystals coated with TATB show the typical feature of well-developed core-shell structure (Figure 1b,c), the 800 nm TATB particles built up a uniform and compact coating shell, with the degree of coverage close to 100%, and almost no free TATB particles can be observed. Surfactants such as PVA and Tween-20 were used to improve the wettabillty of CL-20 and the dispersion of TATB particles. In addition, 2 wt-% of the binder, Estane, was used to favor the immobilization of submicrometer-sized TATB crystals to the Cl-20 surface. With the content of TATB increased from 5 to 25 wt-%, both the coverage and thickness of the TATB shell

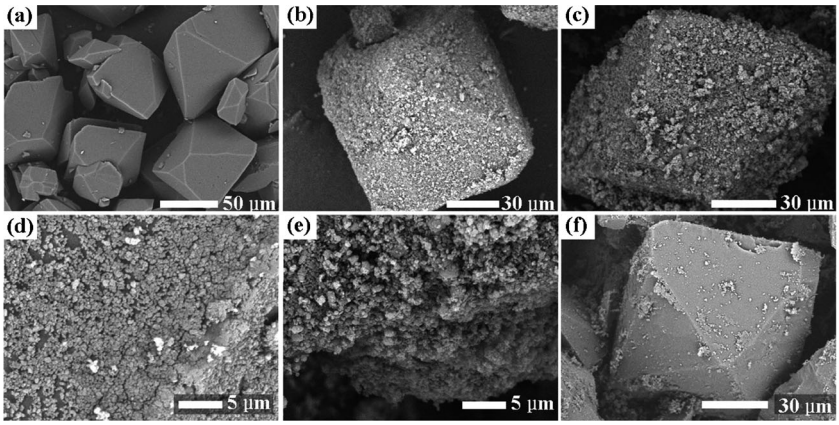

Figure 1. SEM images of CL-20 and CL-20/TATB coated samples: (a) CL-20, (b) 5 wt-% TATB coating, (c) 25 wt-% TATB coating, (d) 5 wt-% TATB coating (high magnification), (e) 25 wt-% TATB coating (high magnification), (f) 5 wt-% TATB physical mixed sample.

were improved. The status of TATB coating on the CL-20 surface could be observed clearly from the SEM images with high magnification (Figure 1d and Figure 1e). For the 5 wt-% TATB coated sample, only very small region of the naked CL-20 crystal surface could be observed, other parts of surface are occupied by the insensitive encapsulation layer. As the content of TATB was increased to 25 wt-%, the whole surface of CL-20 crystal is covered by the rough TATB layer. For comparison, the physical mixtures of CL-20/5 wt-% TATB and Estane binder with the same ratio as those for core-shell structure were prepared as a reference. From the corresponding SEM image (Figure 1f), it is clear that only a small amount of TATB particles were attached to the surface of CL-20, most exist independently, showing negligible coating effect.

By carefully controlling the way of preparation, both the powder and molding powder products of core-shell CL-20/TATB composites can be obtained, which are frequently used in PBXs. Herein, the molding powder products synthesized by bonding of 2 wt-% Estane are spherical, composed of hundreds of CL-20/TATB crystals, with a diameter of about 1 mm (Figure 2a). After pressing in the moulds, such molding powder products can be transformed into explosive pellets with high density, and only such pellets can be used in the practical weapon systems. The pellet density is about 99% of the theoretical density (the possible highest density) after compression, indicating excellent mechanical properties. Besides, no exfoliated dusts were found in the preparation process of explosive pellets, which will benefit the engineering application of this high energy composite.

To further confirm the core-shell structure of CL-20/TATB, a core-etching technique was introduced, which was commonly adopted for the characterization of core-shell materials [32–34]. Herein, ethyl acetate was selected as the etching solvent for CL-20 since TATB is resistant for being dissolved in such system. As shown in Figure 2, after core-etching treatment on the sample with 15 wt-% of coated TATB, the products with hollow TATB shell structure can be clearly identified.

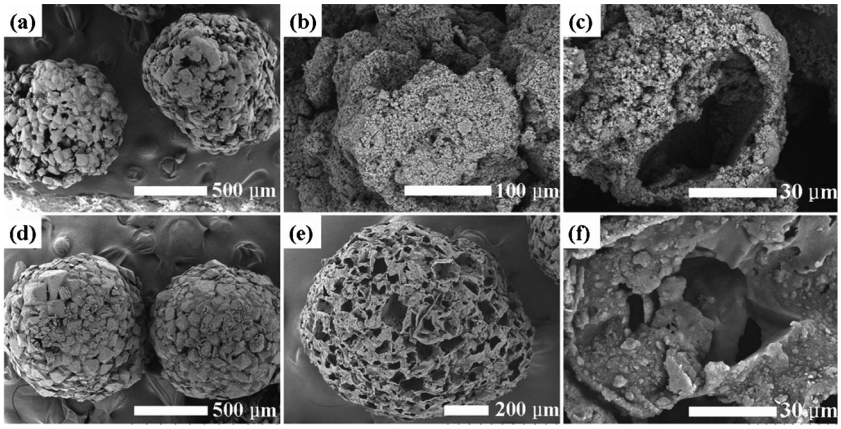

Figure 2. SEM images of CL-20/TATB before and after CL-20 etching: (a) CL-20/TATB + Estane, (b, c) CL-20/TATB + Estane after etching, (d) CL-20/TATB + EVA, (e, f) CL-20/TATB + EVA after etching.

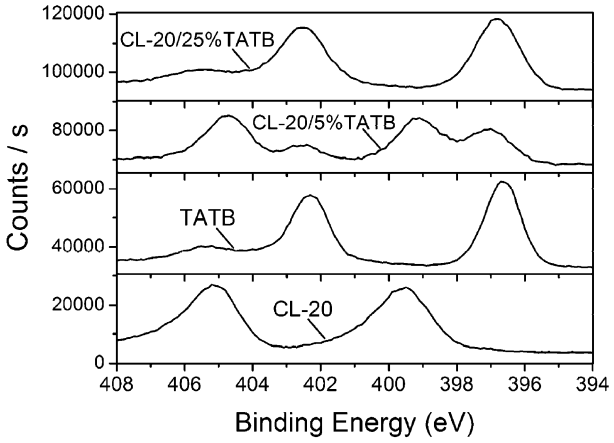

Figure 3. N1s XPS spectrum for CL-20, TATB, and CL-20/TATB core-shell composites. (a) CL-20; (b) TATB; CL-20 coated by (c) 5 wt-% and (d) 25 wt-% TATB.

As ethyl acetate is a good solvent for CL-20, the core was dissolved easily after etching. However, the unexpected solubility of Estane was also found, in this case, the immobilization effect was reduced. A severe collapse of the TATB shell was left, only a part of hollow structure composed of TATB shell can be observed, as shown in Figure 2c. Therefore, 2 wt-% EVA was used as the substitute polymer binder for its insolubility in ethyl acetate. Similar results were obtained for the molding powder products as prepared under the same conditions. However, the TATB coating shell as well as the EVA binder was left intact after etching in spite of the relative low coverage compared to Estane bonded sample. The spherical molding powder presented a honeycomb-like structure after core-etching, the hollow structure of TATB shell is visible, and the thickness of the shell layer can be estimated as 3–10 μm (Figure 2f). Thus, the integrated core-shell structure of CL-20/TATB is verified successfully in this work.

The elemental composition of the core-shell composite surface was measured by XPS. Both CL-20 and TATB contain the elements C, H, O, and N. However, the N1s spectra of these two materials show an obvious difference (Figure 3). For CL-20, the N1s spectrum was resolved into two main peaks with binding energies of 405.2 eV and 399.5 eV, corresponding to the nitro-nitrogen and amine-nitrogen bonds, respectively. For TATB, there are two main peaks centered at 402.3 eV and 396.7 eV, and a secondary peak at 405.2 eV, respectively. The 396.7 eV species belongs to the nitrogen in $-NH_2$ group, the 402.3 eV peak is the main peak from nitrogen in $-NO_2$ group, and the 405.2 eV peak is a satellite one, in accordance with the results as reported recently [35]. The CL-20 sample coated with 5 wt-% TATB displayed a combination of the characteristic peaks of CL-20 and TATB, indicating a certain coating effect. The integrated area ratio of the two peaks with binding energies at 399.5 eV and 396.7 eV is approximately 1 : 1, thus the molecule ratio of TATB:CL-20 on the surface is approximately 2 : 1, indicating an incomplete coating of 5 wt-% TATB with the coverage close to 67 %. As the coating content of TATB was increased to 25 wt-%, the peaks of CL-20 at 405.2 eV and 399.5 eV disappear, only the characteristic peaks of TATB are observed, indicating the excellent coating with the coverage of 100 %. These results are also in good accordance with the SEM analysis as mentioned above. Therefore, the successful fabrication of core-shell structure of CL-20/TATB was further confirmed.

3.2 Sensitivity Study

The results of impact and friction sensitivity studies of the core-shell and physically mixed CL-20/TATB particles are summarized in Table 1, equivalent (2 wt-% of the total weight of the final products) Estane was introduced for each composite. It is known that pure TATB is inert towards both impact and friction due to its graphite-like layered structure [36, 37]. For the physically mixed sample with 5 wt-% TATB, the H_{50} value increased from 16.0 cm to 23.7 cm compared with that of original CL-20. The desensitization was greatly weakened for the poor coverage of TATB, as most of the surface of CL-20 was exposed to the environment. Compared with the TATB/CL-20 mixture, the impact sensitivity for the core-shell CL-20/TATB sample with a similar TATB content is dramatically reduced. The H_{50} value has increased to 49.6 cm, more than three times higher as compared with the original CL-20, implying that the desensitization strategy by core-shell coating is efficient.

With the help of 2 wt-% polymer binder the TATB particles form a compact coating shell. It is known that explosives exhibit high impact sensitivity probably because the "hot spots" grow preferentially with the weak interface of

Table 1. Impact and friction sensitivity of CL-20/TATB composites.

Sample	TATB [wt-%]	TATB introduced	H_{50} [cm]	Friction sensitivity [%]
CL-20	0	–	16.0	100
CL-20/TATB-1	5	physical mixing	23.7	100
CL-20/TATB-2	5	core-shell coating	49.6	68
CL-20/TATB-3	15	core-shell coating	48.2	30
CL-20/TATB-4	25	core-shell coating	56.7	0
CL-20/TATB-5	35	core-shell coating	59.5	4
CL-20/TATB-6	55	core-shell coating	77.6	0

crystals via intervening, spalling, rolling, and smashing [38]. Herein, when CL-20 underwent external impact action, TATB particles coated on the surface were firstly attacked and played a key role for cushion from the impact action. Therefore, fewer hot spots are generated, leading to highly reduced impact sensitivity. Upon increasing the content of TATB, the impact sensitivity of these core-shell CL-20/TATB composites is further decreased. Nevertheless, the extent of reduction became smaller, due to the slow increases in coverage and shell thickness. The H_{50} reaches 77.6 cm as 55 wt-% TATB is adopted.

On the other hand, the friction sensitivity of core-shell CL-20/TATB is reduced to 68% with 5 wt-% TATB, while the value for the physically mixed sample is still 100%. For the core-shell CL-20/TATB composites, the mutual frictions among CL-20 crystals are effectively inhibited. And the friction sensitivity is intensively reduced with increasing content of TATB, due to the graphite-like layered structure and outstanding lubrication effect. As the TATB content is increased to 25 wt-% or more, 0% of friction sensitivity can be obtained.

3.3 Effects of the Amount of Polymer Binder

SEM and sensitivity results of the core-shell CL-20/TATB with different amounts of Estane binder are shown in Figure 4 and Figure 5, respectively (10 wt-% TATB used). It is found that the TATB particles are only partly attached on the surface of CL-20 as 0.5 wt-% Estane was used, causing a low degree of coverage. An amount of 1 wt-% of Estane is sufficient to form the core-shell structure (Figure 4b), and a significant effect could be observed as the amount of Estane was further increased. Similar results were found for EVA bonded samples (not shown). The effects of the polymer binder can be divided in two categories. First, the polymer favors the immobilization and inhibiting the exfoliation of TATB shell. Second, the polymer fills the voids between CL-20 and TATB particles. The latter effect is extremely important for the reduction of impact sensitivity. For example, the unexpected increase of impact sensitivity for the in situ coated HMX by TATB was reported [27], probably due to the hot spots generated from the porous and rough surface of the coated materials. Herein, similar difficulty is well solved by using a small amount of Estane. The H_{50} value rapidly increases with the amount of binder up to 1 wt-%, upon further increasing the amount of polymer has slight influence on the impact sensitivity, as shown in Figure 5. Considering the energy loss derived from the use of excess amount of polymer binder, an amount of 2 wt-% is preferable in view of the coating strength and the maintenance of high energy.

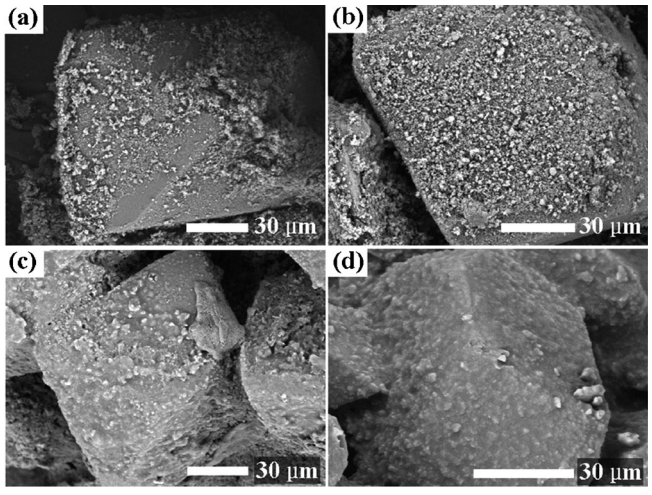

Figure 4. SEM images of core-shell CL-20/TATB with different amount of Estane binder: (a) 0.5 wt-%; (b) 1 wt-%; (c) 2 wt-%; (d) 5 wt-%.

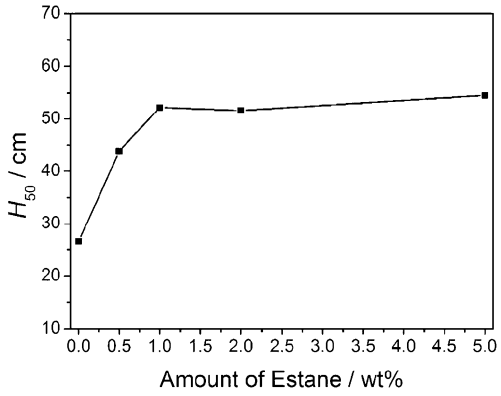

Figure 5. Influence of Estane amount on impact sensitivity.

3.4 Polymorphic Transition Study

CL-20 is well known for its polymorphic transition during the crystallization and application process, especially for the ε to γ form transformation, which caused considerable research interests [39–41]. Crystals of the ε form attracted more attention due to their higher density and energy. XRD analysis [42] was introduced to determine the polymorph of CL-20 used in this work. For ε-CL-20, the space group is $P2_1/a$ and the lattice is monoclinic. Figure 6 shows the XRD patterns of ε-CL-20 and CL-20/TATB composites, the characteristic diffraction peaks (1 1 −1), (2 0 0), and (2 0 −3) of pure CL-20 appear at 2θ of 12.58, 13.83, and 30.31°, respectively. It is clear that the polymorph of CL-20 maintained the optimum ε form after the core-shell coating process. The characteristic peaks of core-shell CL-20/TATB involved the combination of peaks of pure CL-20 and TATB. As the size of TATB particles is in the submicrometer range, the diffraction peaks become slightly broadened. The FT-IR spectroscopic results (not shown) were consistent with those of the XRD analysis. Therefore, it can be concluded that once the CL-20 particles are formed after crystallization, the polymorphic transition of CL-20 is not likely to occur during the

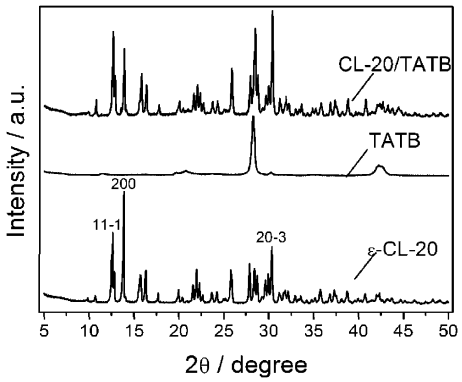

Figure 6. XRD results of the CL-20/TATB composites.

common treatment [40], such as coating of TATB through a water suspension process at 60 °C.

3.5 Thermal Property

Thermal analysis by TG and DSC revealed some interesting phenomena, as depicted in Figure 7 and Table 2. The DSC curve showed an endothermic peak at 161.4 °C and an exothermic peak at 243.0 °C for the original CL-20. They can be attributed to the phase transition from ε to λ form and the characteristic peak for the thermal decomposition of CL-20, respectively [43]. For the physical mixed and core-shell coated CL-20/TATB samples, 2 wt-% Estane was used. A slight shift of these two peaks of the physically mixed CL-20/TATB sample appeared and another exothermic peak at about 370 °C was observed for the composites, which can be ascribed to the thermal decomposition of TATB. In addition, two weight loss stages for the CL-20/TATB composites are evident from the TG results. The weight losses occurred in temperature ranges from 210 to 250 °C and 250 to 380 °C, caused by the decomposition of CL-20 and TATB, respectively. However, a large shift for both peaks could not be ignored for the core-shell coated sample with 10 wt-% TATB. The endothermic peak encountered an increasing shift of 9.3 °C, which could be explained by the increased polymorph thermal stability of CL-20 with the protecting of TATB shell. More interestingly, the decomposition temperature of CL-20 in core-shell samples appears more than 20 °C lower than the original uncoated candidate. This phenomenon might be attributed to the free radicals formed during the depolymerization and thermolysis of Estane, which can further interact with CL-20 and thus cause its easy decomposition. For CL-20 only coated by 2 wt-% Estane, the exothermic peak of appears also more than 20 °C lower than that of pure CL-20. Similar results were reported as a lowering of decomposition temperature of HMX was observed when it was coated with Estane [44, 45]. For PBXs, the use of polymer binder is essential in formulations, and it should be drawn special attention on the possible decrease of the thermal stability of CL-20 caused by such binder. As the coating content of TATB increased to 35 wt-%, the peak for the endothermic phase transition again encountered a shift of 10.4 °C towards higher temperature, while the exothermic decomposition peak returned to 243.5 °C, similar to that of original CL-20. This could be explained by the fact that the TATB content

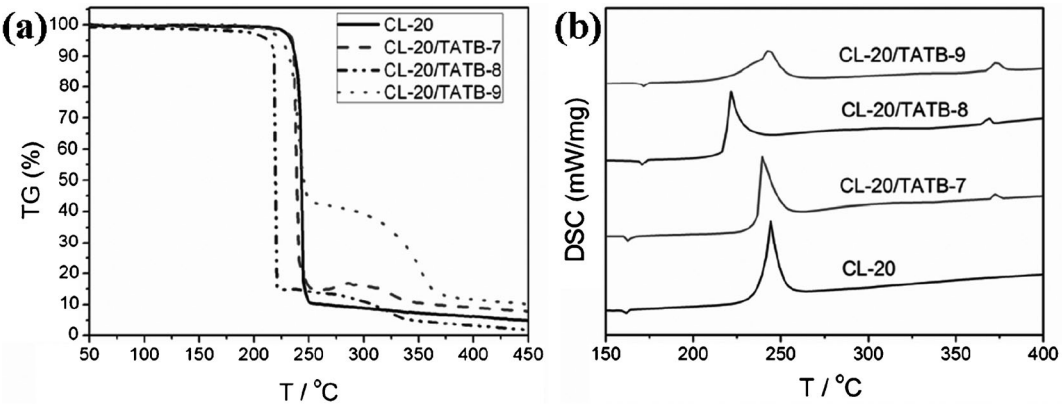

Figure 7. (a) TG and (b) DSC curves of CL-20/TATB composites.

Table 2. Thermal analysis data of CL-20/TATB composites.

Sample	TATB [wt-%]	TATB introduced	endo [°C]	exo[1#] [°C]	exo[2#] [°C]
CL-20	0	–	161.4	243.0	/
CL-20/TATB-7	10	physical mixing	162.6	240.3	372.1
CL-20/TATB-8	10	core-shell coating	170.7	219.6	369.1
CL-20/TATB-9	35	core-shell coating	171.8	243.5	373.8

increased since the free radicals generated from Estane were mainly captured by the thicker TATB shell before their interaction with the inner CL-20 crystals. In order to further improve the thermal stability of such core-shell composites, using polymer binders with better thermal stability is a feasible route.

4 Conclusions

A core-shell assembly of CL-20 crystals with submicrometer-sized TATB with high energy and reduced sensitivity was reported for the first time. An amount of 2 wt-% Estane polymer binder enables a uniform and compact core-shell structure and according to the SEM and XPS results almost 100 % coverage of TATB shell can be achieved. Observation of the hollow TATB shell by etching the CL-20 core in different binder systems confirmed the core-shell structure and the thickness of the TATB shell was estimated to be about 3–10 μm. The binder used for the composites can not only immobilize the TATB particles but also fill the tiny air holes among TATB particles and the voids between CL-20 and TATB. The facile preparation method also enables a controllable shell thickness and easy engineering amplification. Both impact and friction sensitivities are reduced apparently for the coating of 5 wt-% of TATB, and further reduction in sensitivity is realized by increasing the content of TATB. TG and DSC results show that the TATB coating enhances the thermal stability of the polymorph of CL-20, and a higher content used TATB can help to eliminate the influence of free radicals generated from Estane on the exothermic decomposition of CL-20. In addition, the polymorph of CL-20 maintained the optimum ε form after the coating process. Taking into consideration these results, such core-shell assembly strategy provides an efficient route for the desensitization of sensitive explosives while keeping their high energy. The techniques used for the preparation and characterization of core-shell type composites in this work also enrich the knowledge of the materials with similar structural type, especially for the desensitization of high explosives for military applications.

Acknowledgments

This work was supported by the National Natural Science Foundation of China (11202193, 11172276)

References

[1] A. T. Nielsen, M. L. Chan, K. J. Kraeutle, C. K. Lowe-Ma, R. A. Hollins, M. P. Nadler, R. A. Nissan, W. P. Norris, D. J. Vanderah, R. Y. Yee, *Polynitropolyaza-Caged Explosives*, Part 7, *Report NWC TP 7020*, Naval Weapons Center, China Lake, China, November, **1989**.

[2] R. S. Hamilton, A. J. Sanderson, R. B. Wardle, K. F. Warner, Studies of the Crystallization of CL-20, *31st Int. Annual Conference of ICT*, Karlsruhe, Germany, June 27–30, **2000**, 21.

[3] M. Geetha, U. R. Nair, D. B. Sarwade, G. M. Gore, S. N. Asthana, H. Singh, Studies on CL-20: the Most Powerful High Energy Material, *J. Therm. Anal. Calorim.* **2003**, 73, 913.

[4] R. L. Simpson, P. A. Urtiew, D. L. Ornellas, G. L. Moody, K. J. Scribner, D. M. Hoffman, CL-20 Performance Exceeds that of HMX and its Sensitivity is Moderate, *Propellants Explos. Pyrotech.* **1997**, *22*, 249.

[5] J. A. Bumpus, A Theoretical Investigation of the Ring Strain Energy, Destabilization Energy, and Heat of Formation of CL-20, *Adv. Chem. Phys.* **2012**, 1.

[6] N. V. Latypov, U. Wellmar, P. Goede, Synthesis and Scale-up of 2,4,6,8,10,12-Hexanitro-2,4,6,8,10,12-hexaazaisowurtzitane from 2,6,8,10,12-Tetraacetyl-4,10-dibenzyl-2,4,6,8,10,12-hexaazaisowurtzitane (HNIW, CL-20), *Org. Process Res. Dev.* **2000**, *4*, 156.

[7] D. Mueller, New Gun Propellant with CL-20, *Propellants Explos. Pyrotech.* **1999**, *24*, 176.

[8] J. Y. Wang, C. W. An, G. Li, L. Liang, W. Z. Xu, K. Wen, Preparation and Performances of Castable HTPB/CL-20 Booster Explosives, *Propellants Explos. Pyrotech.* **2011**, *36*, 34.

[9] S. S. Samudre, U. R. Nair, G. M. Gore, R. K. Sinha, A. K. Sikder, S. N. Asthana, Studies on an Improved Plastic Bonded Explosive (PBX) for Shaped Charges, *Propellants Explos. Pyrotech.* **2009**, *34*, 145.

[10] R. Sivabalan, G. M. Gore, U. R. Nair, Study on Ultrasound Assisted Precipitation of HNIW and its Effect on Morphology and Sensitivity, *J. Hazard. Mater.* **2007**, *139*, 199.

[11] Y. Bayat, V. Zeynali, Preparation and Characterization of Nano-CL-20 Explosive, *J. Energ. Mater.* **2011**, *29*, 281.

[12] J. Y. Wang, J. L. Li, C. W. An, C. H. Hou, W. Z. Xu, X. D. Li, Study on Ultrasound and Spray-Assisted Precipitation of CL-20, *Propellants Explos. Pyrotech.* **2012**, *37*, 670.

[13] M. H. Lee, J. H. Kim, Y. C. Park, J. H. Hwang, W. S. Kim, Control of Crystal Density of ε-Hexanitrohexaazaisowurzitane in Evaporation Crystallization, *Ind. Eng. Chem. Res.* **2007**, 46, 1500.

[14] X. B. Jiang, X. Y. Guo, H. Ren, Q. J. Jiao, Preparation and Characterization of Desensitized ε-HNIW in Solvent-Antisolvent Recrystallizations, *Cent. Eur. J. Energ. Mater.* **2012**, *9*, 219.

[15] J. Szczygielska, S. Chlebna, P. Maksimowski, W. Skupinski, Friction Sensitivity of the ε-CL-20 Crystals Obtained in Precipitation Process, *Cent. Eur. J. Energ. Mater.* **2011**, *8*, 117.

[16] O. Bolton, A. J. Matzger, Improved Stability and Smart-material Functionality Realized in an Energetic Cocrystal, *Angew. Chem. Int. Ed.* **2011**, *50*, 8960.

[17] D. I. A. Millar, H. E. Maynard-Casely, D. R. Allan, A. S. Cumming, A. R. Lennie, A. J. Mackay, I. D. H. Oswald, C. C. Tang, C. R. Pulham, Crystal Engineering of Energetic Materials: Co-crystals of CL-20, *CrystEngComm* **2012**, *14*, 3742.

[18] Z. W. Yang, H. Z. Li, X. Q. Zhou, C. Y. Zhang, H. Huang, J. S. Li, F. D. Nie, Characterization and Properties of a Novel Energetic–Energetic Cocrystal Explosive Composed of HNIW and BTF, *Cryst. Growth Des.* **2012**, *12*, 5155.

[19] A. Elbeih, A. Husarova, S. Zeman, Path to ε-HNIW with Reduced Impact Sensitivity, *Cent. Eur. J. Energ. Mater.* **2011**, *8*, 173.

[20] J. P. Agrawal. Some New High Energy Materials and their Formulations for Specialized Applications, *Propellants Explos. Pyrotech.* **2005**, *30*, 316.

[21] U. R. Nair, R. Sivabalan, G. M. Gore, M. Geetha. S. N. Asthana, H. Singh, Hexanitrohexaazaisowurtzitane (CL-20) and CL-20-

Based Formulations (Review), *Combust. Explos. Shock Waves* **2005**, *41*, 121.
[22] D. M. Hoffman, Fatigue of LX-14 and LX-19 Plastic Bonded Explosives, *J. Energ. Mater.* **2000**, *18*, 1.
[23] K. J. Kim, H. S. Kim, Coat of Energetic Materials using Crystallization, *Chem. Eng. Technol.* **2005**, 28, 946.
[24] K. J. Kim, H. S. Kim, Agglomeration of NTO on the Surface of HMX Particles in Water-NMP Solvent, *Cryst. Res. Technol.* **2008**, *43*, 87.
[25] J. W. Jung, K. J. Kim, Effect of Supersaturation on the Morphology of Coated Surface in Coating by Solution Crystallization, *Ind. Eng. Chem. Res.* **2011**, *50*, 3475.
[26] G. C. Yang, F. D. Nie, Preparation and Characterization of Core/shell Structure of HMX/NTO Composite Particles, *Sci. Technol. Energ. Mater.* **2006**, *69*, 77.
[27] A. K. Nandi, M. Ghosh, V. B. Sutar, Surface Coating of Cyclotetramethylenetetranitramine (HMX) Crystals with the Insensitive High Explosive 1,3,5-Triamino-2,4,6-trinitrobenzene (TATB), *Cent. Eur. J. Energ. Mater.* **2012**, *9*, 119.
[28] H. Hofmann, K. Rudolf, *Process for the Production of a Pressed Insensitive Explosive Mixture*, US Patent, 2004/0216822 A1, Scully Scott Murphy & Presser, PC, Garden City, NY, USA, **2004**.
[29] C. W. An, F. S. Li, X. L. Song, Surface Coating of RDX with a Composite of TNT and an Energetic-Polymer and its Safety Investigation, *Propellants Explos. Pyrotech.* **2009**, *34*, 400.
[30] C. W. An, J. Y. Wang, W. Z. Xu, Preparation and Properties of HMX Coated with a Composite of TNT/Energetic Material, *Propellants Explos. Pyrotech.* **2010**, *35*, 365.
[31] National Military Standard of China, *Experimental Methods of Sensitivity and Safety*, GJB/772A-97, **1997** (in Chinese).
[32] N. Ren, Z. J. Yang, X. C. Lv, J. Shi, Y. H. Zhang, Y. Tang, A Seed Surface Crystallization Approach for Rapid Synthesis of Submicron ZSM-5 Zeolite with Controllable Crystal Size and Morphology, *Microporous Mesoporous Mater.* **2010**, *131*, 103.
[33] Y. T. Zhong, X. Wang, K. C. Jiang, J. Y. Zheng, Y. G. Guo, Y. Ma, J. N. Yao, A Facile Synthesis and Lithium Storage Properties of Co_3O_4–C Hybrid Core-shell and Hollow Spheres, *J. Mater. Chem.* **2011**, *21*, 17998.
[34] G. Z. Chen, S. Desinan, R. Rosei, F. Roseia, D. L. Ma, Hollow Ruthenium Nanoparticles with Small Dimensions Derived from Ni@Ru Core@shell Structure: Synthesis and Enhanced Catalytic Dehydrogenation of Ammonia Borane, *Chem. Commun.* **2012**, *48*, 8009.
[35] J. A. Carter, J. M. Zaug, A. J. Nelson, M. R. Armstrong, M. R. Manaa. Ultrafast Shock Compression and Shock-induced Decomposition of 1,3,5-Triamino-2,4,6-trinitrobenzene Subjected to a Subnanosecond-duration Shock: An Analysis of Decomposition Products, *J. Phys. Chem. A* **2012**, *116*, 4851.
[36] W. H. Zhu, H. M. Xiao, First-principles Bandgap Criterion for Impact Sensitivity of Energetic Crystals: A Review, *Struct. Chem.* **2010**, *21*, 657.
[37] M. B. Talawar, A. P. Agarwal, M. Anniyappan, G. M. Gore, S. N. Asthana, S. Venugopalan, Method for Preparation of Fine TATB (2–5 μm) and its Evaluation in Plastic Bonded Explosive (PBX) Formulations, *J. Hazard. Mater.* **2006**, *137*, 1848.
[38] X. L. Song, Y. Wang, C. W. An, X. D. Guo, F. S. Li, Dependence of Particle Morphology and Size on the Mechanical Sensitivity and Thermal Stability of Octahydro-1,3,5,7-tetranitro-1,3,5,7-tetrazocine, *J. Hazard. Mater.* **2008**, *159*, 222.
[39] Y. T. Lapina, A. S. Savitskii, E. V. Motina, N. V. Bychin, A. A. Lobanova, N. I. Golovina, Polymorphic Transformations of Hexanitrohexaazaisowurtzitane, *Russ. J. Appl. Chem.* **2009**, *82*, 1821.
[40] J. C. Gump, S. M. Peiris, Phase Transitions and Isothermal Equations of State of ε-Hexanitrohexaazaisowurtzitane (CL-20), *J. Appl. Phys.* **2008**, *104*, 083509–1.
[41] J. Li, T. B. Brill, Kinetics of Solid Polymorphic Phase Transitions of CL-20, *Propellants Explos. Pyrotech.* **2007**, *32*, 326.
[42] H. X. Chen, S. S. Chen, L. J. Li, S. H. Jin, Quantitative Determination of ε-Phase in Polymorphic HNIW Using X-ray Diffraction Patterns, *Propellants Explos. Pyrotech.* **2008**, *33*, 467.
[43] R. Turcotte, M. Vachon, Q. S. M. Kwok, R. P. Wang, D. E. G. Jones, Thermal Study of HNIW (CL-20), *Thermochim. Acta* **2005**, *426*, 105.
[44] G. Singh, S. P. Felix, P. Soni, Studies on Energetic Compounds Part 28: Thermolysis of HMX and its Plastic Bonded Explosives Containing Estane, *Thermochim. Acta* **2003**, *399*, 153.
[45] A. K. Burnham, R. K. Weese. Kinetics of Thermal Degradation of Explosive Binders Viton A, Estane, and Kel-F, *Thermochim. Acta* **2005**, *426*, 85.

Received: February 2, 2013
Revised: April 30, 2013
Published online: June 20, 2013

